# Ultrafast probes of nonequilibrium hole spin relaxation in the ferromagnetic semiconductor GaMnAs

Aaron Patz, Tianqi Li, Xinyu Liu, Jacek K. Furdyna, Ilias E. Perakis, and Jigang Wang

Phys. Rev. B **91**, 155108 — Published 8 April 2015

DOI: 10.1103/PhysRevB.91.155108

# Ultrafast Probes of Nonequilibrium Hole Spin Relaxation in Ferromagnetic Semiconductor GaMnAs

A. Patz,[1] T. Li,[1] X. Liu,[2] J. K. Furdyna,[2] I. E. Perakis,[3] and J. Wang[1]

[1] *Ames Laboratory - USDOE and Department of Physics and Astronomy, Iowa State University, Ames, Iowa 50011, USA*
[2] *Department of Physics, University of Notre Dame, Notre Dame, Indiana 46556, USA*
[3] *Department of Physics, University of Crete and Institute of Electronic Structure & Laser, Foundation for Research and Technology-Hellas, Heraklion, Crete, 71110, Greece*

(Dated: March 19, 2015)

We report direct measurements of hole spin lifetimes in ferromagnetic GaMnAs carried out by time- and polarization-resolved spectroscopy. Below the Curie temperature, ultrafast photoexcitation of GaMnAs with *linearly-polarized* light is shown to create a non-equilibrium hole spin population via dynamical polarization of the holes through *p-d* exchange scattering with ferromagnetically-ordered Mn spins. The system is then observed to relax in a distinct three-step recovery process: (i) a femtosecond hole-spin relaxation, on the scale of 160-200 fs, (ii) a picosecond hole-energy relaxation, on the scale of 1-2 ps, and (iii) a coherent, damped Mn spin precession with a period of 250 ps. The transient amplitude of the hole-spin relaxation component diminishes with increasing temperature, directly following the ferromagnetic order of GaMnAs, while the hole-energy amplitude shows negligible temperature change. Our results serve to establish the hole spin lifetimes in the ferromagnetic semiconductor GaMnAs, at the same time demonstrating a novel spectroscopic method for studying non-equilibrium hole spins in the presence of magnetic order and spin exchange interaction.

## I. INTRODUCTION

Spin exchange, fluctuation and relaxation play important roles in various collective behaviors emerging in advanced materials with scientific interest and technological potential, such as carrier-mediated ferromagnetism in semiconductors, colossal magnetoresistance in manganites, and electronic nematicity in iron pnictide superconductors[1–3]. These processes develop on ultrafast time scales and can be driven and probed by ultrashort laser pulses interacting with magnetic materials. Revealing the associated nonequilibrium spin dynamics provides additional information, beyond time-averaged properties obtained from static measurements, to both understand and to control these phenomena.

Recently, nonequilibrium hole spin dynamics in semiconductors has emerged as an important issue. For example, in *p*-type doped GaAs, the spin-polarized holes photoexcited by circularly polarized mid-infrared pulses were shown to exhibit an ultrafast exponential decay with a spin lifetime of 110 femtoseconds (fs) at room temperature[4]. In contrast, a substantially longer hole spin relaxation time, on the order of hundreds of picoseconds (ps), was inferred from spin tunneling and transport experiments in ferromagnetic *p*-Si and *p*-Ge heterostructures[5–7]. Furthermore, in bulk Ge, hole spin lifetimes are reported to differ by two orders of magnitude (700fs vs. 100ps) although some reconciliation was found in that the hole-spin relaxation rate decreased with lower temperature and/or excitation density[8,9]. However, a unified understanding of the wide range of hole spin lifetimes observed in semiconductors is still missing, and more measurements are clearly desirable in complementary systems, including magnetically-doped semiconductors. In addition to its scientific value, comprehensive and reliable knowledge of hole spin lifetimes are also important for the development of spin computation and communication technology based on conducting holes and/or electrons[10–12].

So far, hole spin relaxation has only been studied in weakly-interacting spin ensembles without long-range magnetic order, e.g., *p*-GaAs, *p*-Si, *p*-Ge. However, (III,Mn)V magnetic semiconductors displaying carrier-mediated ferromagnetism, such as GaMnAs, represent a model system for investigating hole spins influenced by ferromagnetic order and spin exchange interaction. For example, magnetic coupling between impurity band holes arising from Mn-doping and localized Mn spins in GaMnAs strongly depends on the hole density, spin polarization, and distribution among the bands[13].

The work presented here was motivated by previous time-resolved studies of ultrafast spin dynamics and magnetization control in the (III,Mn)V magnetic semiconductors. This includes femtosecond Mn spin canting induced by spin-orbit torques[14,15] via photoexcited non-thermal "transverse" hole spins involving the interplay between spin–orbit and magnetic exchange interaction[16,17]; femtosecond demagnetization (i.e. decrease of Mn spin amplitude) via dynamical polarization of "longitudinal" holes spins[18–20]; picosecond photoinduced ferromagnetism[21]; and magnetization precession[22–28].

However, despite extensive studies in these (III,Mn)V ferromagnetic semiconductors, hole spin relaxation time is yet to be determined, and the distinction between nonequilibrium hole spin relaxation and hole energy relaxation still need to be explored. In this case, the absence of conclusive observations is due in part to the lack of experimental techniques that can generate and probe spin-polarized holes at femtosecond time scales, especially in

heavily hole-doped materials.

In this paper we report the observation of femtosecond hole spin relaxation in the ferromagnetic semiconductor, GaMnAs, using degenerate ultrafast magneto-optical Kerr (MOKE) spectroscopy. These measurements reveal a femtosecond demagnetization followed by a fast and a slow recovery of the transient MOKE signal. Importantly, the fast recovery appears only in the magnetically-ordered state, and it is characterized by a temperature-dependent transient amplitude that closely tracks the ferromagnetic order and vanishes at the Curie temperature. In contrast, the slow recovery persists in the paramagnetic phase, and its transient amplitude shows negligible temperature dependence. From this observation we infer that the optical nonlinearity of the fast component is determined by the dynamical polarization of hole spins due to scattering with the magnetically-ordered Mn ion spins through $p$-$d$ exchange scattering. Consequently, this component provides a direct measurement of the characteristic hole spin (HS) lifetimes in GaMnAs of $\tau_{HS}$ ∼160-200 fs.

The HS component is distinguished in time from the subsequent decay of the Kerr rotation amplitude attributed to hole energy (HE) relaxation, and characterized by $\tau_{HE}$ ∼1-2ps. Finally, on much longer timescales, a coherent damped Mn spin precession is observed, with a period of ∼250 ps at zero external magnetic field. Our results thus reveal different three different stages of spin dynamics in a magnetic semiconductor. We note parenthetically that the use of near-infrared linearly polarized pulses represents a new approach for creating and studying a non-equilibrium hole spin population in the presence of ferromagnetic order, and it is much simpler to implement than techniques based on mid-infrared circularly polarized pulses[4,8,9,20,29].

## II. EXPERIMENTAL AND SAMPLE DETAILS

The photoinduced magnetization dynamics of our GaMnAs sample were studied via ultrafast MOKE spectroscopy, as follows. A 1.0 KHz Ti:Sapphire laser amplifier was used to generate pulses at a central wavelength of 800nm and a pulse durations of 35fs. The output pulses were separated into two beam paths serving as the pump and probe. Both beams were linearly polarized. A chopper modulated the pump beam at a frequency of 500Hz. After reflecting from the sample, the probe beam was passed through a polarization bridge and was measured with a balanced photodetector and lock-in amplifier. In the polar geometry used here, the Kerr rotation angle, $\Delta\theta$, is proportional to the out-of-plane magnetization $M_Z$ of the sample.

Our sample was a 70nm $Ga_{0.925}Mn_{0.075}As$ (GaMnAs) thin film deposited by low-temperature molecular beam epitaxy (MBE) on a GaAs buffer layer on top of a semi-insulating (001) surface of a GaAs substrate. The Curie temperature and hole density of our specimen were 77 K and $3 \times 10^{20}$ cm$^{-3}$, respectively. The ultrafast laser measurements were performed in a liquid helium cooled cryostat.

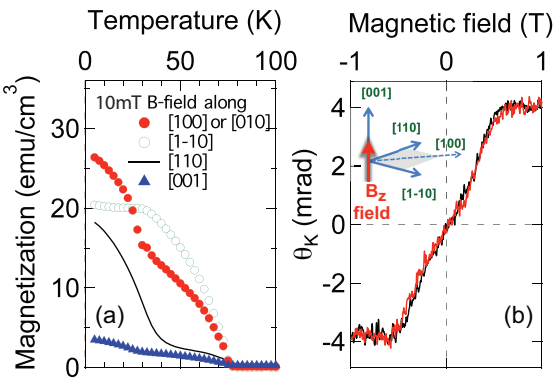


FIG. 1: (a) Temperature dependence of static magnetization along four different directions of our GaMnAs sample; [100] or [010] (red solid circles), [1$\bar{1}$0] (green hollow circles), [110] (black line) and [001] (blue triangles). (b) Static MOKE angle $\theta_k$ at 5K measured in polar geometry with external field B nearly along the [001] direction (∼5deg away). Coordinate system is defined in the inset.

At low temperatures, spontaneous magnetization from the carrier-mediated ferromagnetic order naturally aligns along one of the two equivalent, orthogonal easy axes lying in the sample plane close to the [100] and [010] crystallographic axes. As the temperature is increased to above $T_R$ ∼ 30K, changes occur in the anisotropy field in the GaMnAs specimen, such that the easy axis now reorients to near the [1$\bar{1}$0] direction. This reorientation is illustrated in Fig. 1(a), showing magnetization of the GaMnAs sample observed along four different directions in an external magnetic field of $B_{ext}$ ∼10mT. The coordinate system which we use is defined in the inset of Fig. 1(b). Fig. 1(b) shows static MOKE measurements carried out at T=5K as a function of external magnetic field $B_{ext}$ applied in the polar geometry, i.e., along the [001] axis, as shown in the inset. An increasing MOKE signal $\Theta_K$ is observed up to ∼500mT, where the magnetization saturates. In our ultrafast measurements discussed later, an external magnetic field of $B_{ext} \sim 250mT$ is applied along [001] (defined as the z-direction) unless labelled otherwise. The direction of the resultant magnetization of the sample is always determined by the combination of the external field and the internal anisotropy fields.

Fig. 2 illustrates the origin of the static and ultrafast MOKE signals in GaMnAs for T<$T_C$. The linearly polarized probe beam with photon energy of 1.55eV strongly couples to the electronic transition across the direct band-gap at the Γ-point. The valance bands are spin-split due to strong exchange coupling with the ferromagnetically-aligned Mn spins in $d$-like states (shown in gold) that hybridize with the upper valence band, as shown in Fig. 2(a). The size of the splitting is proportional to the magnetization of the Mn ions and

forms the mean-field gap $\Delta_{MF}$. The holes occupy these bands up to the Fermi energy, as discussed by Dobrowolska *et al.*[13]. The conduction bands, on the other hand, are barely affected by the Mn spins due to their *s*-like symmetry and weak *s*–*d* coupling. According to the optical selection rule $\Delta J = \pm 1$, the right ($\sigma_+$) and left ($\sigma_-$) circularly polarized components of the incident linearly-polarized probe light couple to electronic transitions from the spin-polarized valence bands to the degenerate conduction band with opposing spins. Consequently, the origin of the static (no pump) MOKE signal below $T_C$ is caused by the difference in the refractive indices corresponding to the opposite circular polarizations of the two branches of light, which is proportional to $\Delta_{MF}$.

The main focus of this paper is to apply a time-resolved MOKE technique in order to obtain key information about the coupling between different reservoirs (electronic, spin, etc...) and their dissipation by measuring the recovery of the non-equilibrium state following femtosecond pump excitation. Upon ultrafast pump excitation at 1.55eV, hot holes become photoexcited out of equilibrium, giving rise to a blurred Fermi surface at such fast timescales. Due to the strong exchange interaction between the hole and the Mn ion spins, the photoexcitation results in a transfer of angular momentum from ferromagnetically-ordered Mn to the hot holes. This in turn quasi-instantaneously demagnetizes the Mn ions and creates an initial non-equilibrium spin-polarized hole state even under linearly-polarized laser excitation at temperatures below $T_C$. This ultrafast demagnetization (as measured by the change of the MOKE amplitude $\Delta_K$) of (III,Mn)V materials has been interpreted as the reverse of the Overhauser effect; i.e. where the excited holes become dynamically spin polarized at the expense of the localized Mn spins[19,20]. To study this non-equilibrium photo-excited hole state, we use a degenerate pump/probe method where the probe energy is chosen to have the same energy as the pump, at 1.55eV, which then directly couples to the transient carrier population.

Figure 2(b) illustrates the three interconnected relaxation processes that contribute to the observed *ultrafast* MOKE response following the linearly-polarized pump pulse excitation. The three relaxation processes are denoted by yellow arrows marked as 1,2,3. The first process is the relaxation of transient spin-polarized holes, which scatter between the spin-split valence bands. Note that a similar relaxation does not occur for the photoexcited conduction electrons, because the linearly polarized pump pulse does not transfer any net angular momentum, and therefore does not create any net electron spin. Additionally, there is no preferred spin orientation for the photoexcited conduction electrons to which they can relax.

The second process is that of the energy relaxation of the transient hot holes, which can be understood as cooling via phonon scattering towards zone center of the valence and impurity bands. Although there is no change of the spin polarization, this process contributes to the transient MOKE signals by altering the absorption coefficients for both circular polarizations, commonly referred to as dichroic bleaching in studies of ferromagnetic metals[30,31]. The third relaxation process corresponds to coherent Mn spin precession and its Gilbert damping via spin-lattice scattering. The latter two processes have been reported and discussed in earlier studies (citation needed here) whereas the hole-spin dynamics have not been previously investigated.

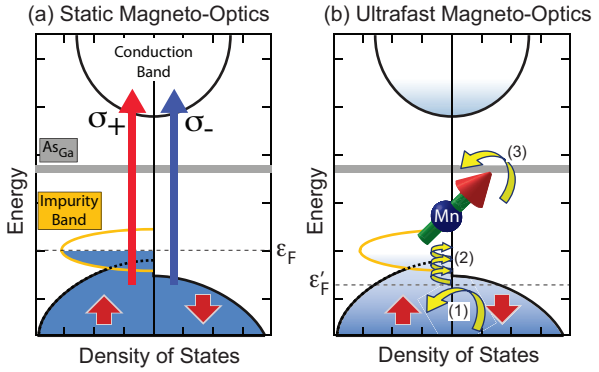


FIG. 2: Energy level diagram of GaMnAs. (a) The static MOKE signal at $\hbar\omega = 1.55eV$ arises from the difference in the refractive indices of the two circularly polarized components of incident light ($\sigma_+$ drawn as red arrow, $\sigma_-$ as blue arrow). The *d*-like electronic orbitals of Mn form a dispersion-less, mid-gap impurity band (shown in gold) that hybridizes with the upper valence band[13]. Red arrows inside the conduction band indicate spin up/down bands. (b) Yellow arrows mark the three relaxation processes observed after ultrafast photoexcitation. Equilibrium or quasi-equilibrium Fermi levels after photoexcitation are shown as dashed lines. These processes are: (1) hole spin-flip relaxation via scattering between the spin split valence bands; (2) hot hole energy relaxation via phonon scattering within the valence and impurity band; and (3) coherent Mn spin precession and Gilbert damping.

## III. RESULTS AND ANALYSIS

A typical trace of ultrafast photoinduced MOKE rotation -$\Delta\theta_k$ data taken at 4K is shown in Fig. 3(a). In the figure, the x-axis is split to show short- and long-time dynamics. There is an initial $\sim 40fs$ reduction of the MOKE amplitude (inset) due to femtosecond demagnetization that leads to a negative change in the ultrafast MOKE signal. Subsequently, a distinct three-step recovery of $\Delta\theta_k$ is observed, consistent with Fig. 2(b). The relaxation processes are labeled in the figure as (1) a fast decay (corresponding to $\tau_{HS} \sim 200fs$), (2) a slow decay ($\tau_{HE} \sim 2ps$), and (3) a periodic oscillation with a period of $\sim 250ps$ superimposed on a much slower Gilbert relaxation. We discuss these three processes in detail in the sections that follow.

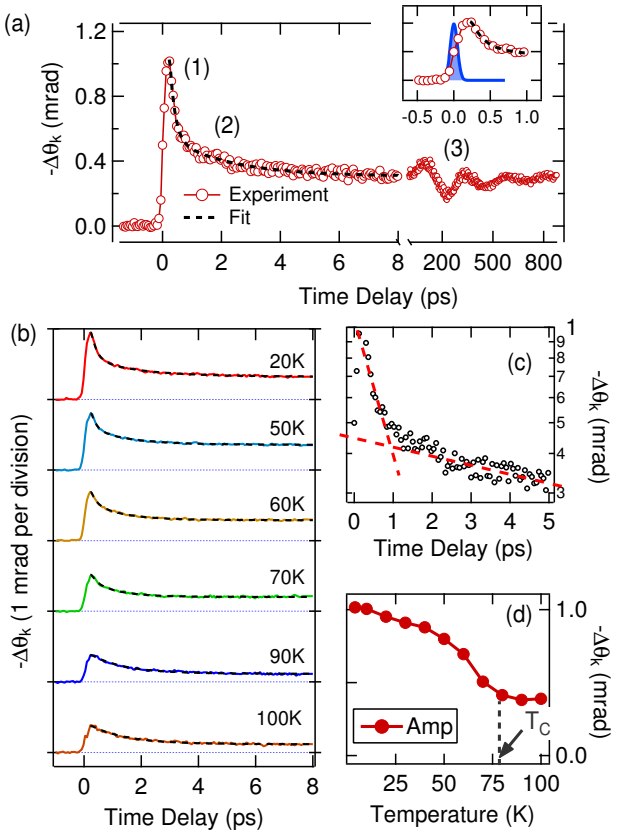


FIG. 3: (a) A representative trace of the low temperature data (taken at 4K) shown with a split x-axis. Following an ultrafast negative rise of $\Theta_K$ (demagnetization), a three-step recovery of the MOKE signal is clearly seen, characterized by (1) fast, $\sim 200fs$; (2) slow, $\sim 2ps$ time constants, followed at longer timescales by (3) a periodic oscillation superimposed upon a much slower decay at a time scale of hundreds of picoseconds. The inset shows the cross-correlation of pump and probe (blue fill). (b) Temperature dependence of the MOKE dynamics during the first 8ps at various temperatures. The traces are vertically offset for clarity. Black dashed lines overlaid on the data show the bi-exponential fitting, as illustrated in (c) by a semilogarithmic plot of the 4K trace in (c). Red dashed-lines in (c) mark the two decay components. (d) Peak amplitude of the ultrafast photoinduced MOKE rotation as a function of temperature. The Kerr measurements were made with a magnetic field of $B_{ext} \sim 250$mT applied perpendicular to the sample during, and with a pump fluence of $\sim 690 \mu J/cm^2$.

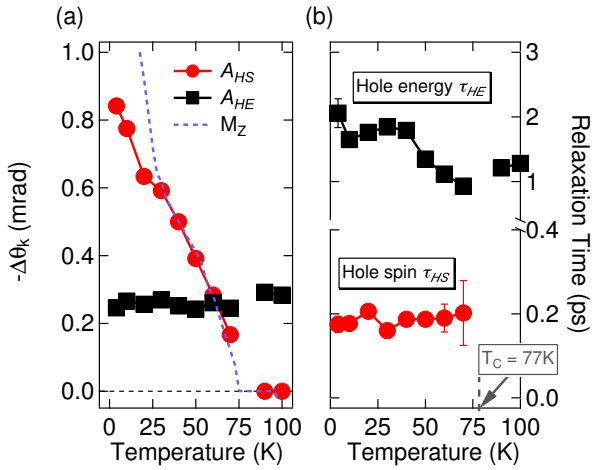


FIG. 4: (a) Transient amplitude $A_{HS}$ (red) extracted from Eq. (1) for the hole-spin relaxation process, and its scaling with the static magnetization along [001] (blue dashed line) for temperatures above $T_R \sim 30$K (i.e. where the easy axis reorientation occurs), and the amplitude of the hole-energy relaxation, $A_{HE}$ (black), remains mostly constant with temperature. (b) Relaxation times as a function of temperature for the $\tau_{HS}$ (red) and $\tau_{HE}$ components (black).

### A. Short-time dynamics: hole spin and energy relaxation

We first turn the reader's attention to the partial recovery of the MOKE signal within the first few ps after photoexcitation, shown in Fig. 3(b). The fast dynamics largely reflects the relaxation of the photoexcited holes. Careful inspection of the Kerr data shows that the fast time-scale recovery process is in the form of a bi-exponential relaxation, clearly seen in the semi-logarithmic plot shown in Fig. 3(c), where two red dashed lines are overlaid on the T=4K Kerr data.

Ultrafast MOKE measurement results for various temperatures from 20K to 100K are presented in Fig. 3(b), showing the main features of the fast relaxation dynamics at different temperatures.Importantly, below $T_C$=77K, the data show bi-exponential decay, corresponding to $\tau_{HS}$ and $\tau_{HE}$ relaxation components, while above $T_C$ the signal shows only a single exponential decay with only the slower $\tau_{HE}$ component. After crossing into the paramagnetic phase the macroscopic spin order is no longer present, and thus there also are no dynamically polarized hole spins. In addition, since linearily polarized pumping does not deposit any net angular momentum, one expects to only observe the hole spin relaxation below $T_C$. We can therefore attribute the slower component $\tau_{HE}$ to hole energy relaxation. On the other hand, since the femtosecond component $\tau_{HS}$ disappears at temperatures above $T_C$, we ascribe it to hole spin relaxation (further support of this is discussed below). Additionally, in the inset of Fig 3(a) we present the T=4K $\Delta\Theta_K$ trace alongside the pump-probe cross-correlation (blue fill) to illustrate that the fast $\tau_{HS}$ relaxation is indeed temporally resolvable with our pulse duration, and is not due to a coherent interaction between the pump and the probe beams[32,33].

Furthermore, as shown in Fig. 3(d), the peak amplitude of the photoinduced MOKE signal decreases with increasing temperature up to $T_C$, although the signal persists even above above the transition temperature. This behavior indicates that the ultrafast MOKE signal contains contributions from both the ferromagnetic order

and from non-equilibrium hole spin and charge populations, as discussed in the prior section. As seen in Figs. 3 and 4, the transient MOKE amplitude is constant above $T_C$, which further corroborates our assignment of the slower component $\tau_{HE}$ to hole energy relaxation.

For quantitative analysis, we fit the observed short time dynamics with a bi-exponential decay function convoluted with the probe pulse. The temperature dependent fittings are shown overlaid on the data in Fig. 3(a,b) (black, dashed-lines). The bi-exponential fitting function is given by:

$$f(t) = A_{HS}\ e^{(-t/\tau_{HS})} + A_{HE}\ e^{(-t/\tau_{HE})} + A_C \qquad (1)$$

$\tau_{HS}$ and $\tau_{HE}$ are the characteristic decay time constants for the hole-spin and hole-energy relaxation processes, and $A_{HS}$ and $A_{HE}$ are their respective transient amplitudes. The third term represents the long-time Mn spin-relaxation and other possible non-magnetic long-time contributions. These contributions are practically time-independent over the 8ps scale considered in the fitting, and are therefore represented as a constant, $A_C$ in Eq. (1).

Figure 4(a,b) shows the temperature dependence of the parameters obtained from the above fitting. The amplitude of the hole spin component $A_{HS}$ (red dots) diminishes with increasing temperature, and disappears above $T_C$, closely tracking the static magnetization curve along [001] (dashed blue line) shown for comparison in Fig. 4(a)[34]. The reason that the $A_{HS}$ closely tracks the ferromagnetic order can be explained in terms of the reverse-Overhauser effect, which is the process where the holes acquire angular momentum from the Mn ions. When the initial magnetization of the Mn ions is larger, more net angular momentum is transferred to holes. Subsequently, as holes relax to equilibrium, they must return this excess angular momentum via the hole spin relaxation process (labeled '1' in Fig. 2(b)). In the case of larger initial magnetization, $A_{HS}$ will also be larger because $A_{HS}$ reflects the amount of angular momentum being lost by the holes in this process. The slight discrepancy at temperatures below $T_R$ ∼30K likely originates from the spin reorientation process, which will be discussed in the next subsection.

On the other hand, $A_{HE}$ (black squares) remains constant throughout the entire temperature range, and persists above $T_C$. This behavior corroborate our conclusions regarding the magneto-optical nonlinearities of the MOKE signals, indicating that the magnetization-dependent amplitude $A_{HS}$ measures the contribution of the spin-polarized hole population generated via dynamical polarization transfer from the macroscopic magnetization of the Mn ions to the holes. Thus the corresponding decay time $\tau_{HS}$ measures the hole spin relaxation time, while the non-magnetic amplitude $A_{HE}$ describes the hot hole population independent of $T_C$, and its corresponding decay time $\tau_{HE}$ represents hot hole energy relaxation in the valence and Mn-impurity bands via phonon emission.

The fast hole-spin decay time $\tau_{HS}$ (red solid dots) remains approximately constant at ∼160-200fs between 4K and $T_C$, as shown in Fig. 4(b). These directly measured values are consistent with an upper bound value ∼200fs estimated from earlier femtosecond demagnetization experiments on (III,Mn)V ferromagnetic semiconductors[20]. These values are slightly larger than the ∼50–80fs predicted theoretically for GaMnAs at low temperatures[35]. In these materials, the fast hole spin-relaxation can be attributed to spin-orbit coupling in the valence band mediated by ultrafast momentum scattering in the excited states that gives rise to a strongly fluctuating spin-orbit field acting on hole spins. This results in very fast and temperature-independent femtosecond decay in the ferromagnetic phase, which is likely to be more efficient than any other relaxation mechanism that leads to temperature dependence as predicted[35].

The hole energy relaxation time $\tau_{HE}$ (black squares in Fig. 4b) remains constant up to around the easy axis reorientation temperature $T_R$ ∼ 30-40K, where it begins to decrease, exhibiting a downward cusp near $T_C$. This interesting behavior, showing some dependence on the magnetization, is not understood, but it may originate from a strong, magnetization-dependent mixing between the valance band and the Mn $d$ band and/or the complicated spin-induced renormalization of the hole states[36,37].

The observed relaxation time $\tau_{HE}$ of ∼1-2ps is consistent with hole energy relaxation times measured earlier in GaMnAs, and our present results further reveal its non-trivial temperature dependence that shows some influence of the ferromagnetic state of the material. A different process with a similar relaxation time ∼ 1ps has been observed previously, and has been attributed to trapping of photoexcited electrons by crystal defects, with no relation to the magnetic system[38–40]. Our present results thus point to a need for future studies aimed at a better understanding of the hole-energy dynamics occurring in ferromagnetic semiconductors.

### B. Long-time dynamics: coherent Mn spin precession

In this section we briefly discuss the coherent oscillatory behavior of Mn spins observed via the $\Delta\theta_k$ signal on the scale of hundreds of picoseconds in these experiments, similar to effects already reported in the literature[22–28]. In order to isolate Mn-related dynamics without contribution from hole dynamics, we use a low pump fluence and a two-color method of ultrafast MOKE spectroscopy, i.e., we now tune the pump to 3.1eV so as to couple to energies far away from the Fermi level at the Γ-point. This allows us to avoid the overshoot behavior related to hole spin and energy dynamics discussed in the preceding section.

At zero magnetic field and well below $T_C$, the initial magnetization direction is close to the [100] easy axis in

the plane of the sample as shown in Fig. 1(a). The magnetization dynamics triggered by the femtosecond laser pulse excitation is shown in Fig. 5(a). Here the main feature is the oscillation of the Kerr signal caused by the oscillatory component of magnetization $M_Z$ due to the collective precession of the magnetization around its in-plane equilibrium orientation at a frequency of ~4.2 GHz (see inset), as discussed in the literature[22–28]. The observed precession frequency in the low field limit is well described analytically by the formula,

$$\omega_m = \gamma \cdot \sqrt{H_{4\parallel} \cdot (H_{2\perp} + H_{4\parallel})} \qquad (2)$$

where $H_{2\perp}$ and $H_{4\parallel}$ represent the effective uniaxial and cubic anisotropy fields, respectively. The quantities $H_{2\perp}$ and $H_{4\parallel}$ are defined in terms of anisotropy energies $K_i$ as $4\pi M - \frac{2K_{2\perp}}{M}$ and $\frac{2K_{4\parallel}}{M}$. From the experimental magnetization curve measured along the hard axis shown in Fig. 1(b) we estimate $H_{2\perp}$ and $H_{4\parallel}$ for our sample to be 0.3T and 0.06T at 5K, which yields a precession frequency $\omega_m = 4.12GHz$, in good agreement with our measured data. In addition, our results in Fig. 5(b) show that the spin precession is no longer observed when the perpendicular B field increases to 1T. This can be understood as follows. At this high field the magnetization becomes fully aligned along the B-field (i.e., along the [001] direction), and the precession of magnetization is undetectable through $\Theta_K$). We attribute the conspicuous negative shift in $\Theta_K$ seen in Fig. 5(b) seen upon photoexcitation to so-called laser-induced ultrafast demagnetization, i.e., photoinduced femtosecond changes in total magnetization amplitude.[18,20]

Returning to the Kerr results observed at B=0, the observed precession (seen as $\Delta\Theta_K$) is triggered by the pump-induced transient change of the easy axis that results from the competition between uniaxial $[1\bar{1}0]$ and cubic [100] anisotropy fields. As shown in Fig. 1(a), the magnetization in the sample naturally aligns along the easy axis established by the dominant anisotropy field, which at low temperatures is close to [100]. At these low temperatures, thermal effects due to the pump pulse manifest themselves as a strengthening of the uniaxial field along $[1\bar{1}0]$ relative to the cubic anisotropy field along [100], equivalent to a change of the easy axis direction towards $[1\bar{1}0]$. This induces precession of the magnetization along the new easy axis direction, consistent with the oscillations observed in the z-direction, as shown in the 5K, 20K and 25K traces in Fig. 5(c). Above the easy-axis reorientation temperature $T_R$ ~30K, the uniaxial anisotropy field becomes dominant, as seen in temperature dependence of static magnetization along four different directions in Fig. 1(a), and the magnetization aligns along the $[1\bar{1}0]$ direction. Thermal effects which strengthen this field, cannot induce precession of the magnetization anymore, as evident by the disappearance of the oscillations above this reorientation temperature. In addition, below this temperature the strong cubic anisotropy field associated with the [100] direction

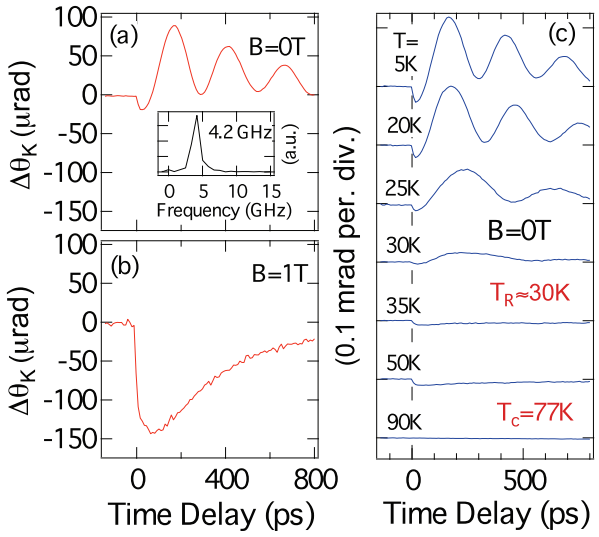


FIG. 5: (Color online) Ultrafast non-degenerate MOKE measurements at 0T (a) and 1T (b). T=4K and pump/probe photon energy is set to 1.55eV/3.1 eV. Inset shows the 0T oscillation spectrum. (c) The temperature dependence of ultrafast non-degenerate MOKE signals at various temperatures and traces are vertically offset for clarity. The pump fluence is ~7$\mu$J/cm$^2$.

makes the magnetization vector tilt from the z-axis below $T_R$, which explains the slight deviation between the static magnetization and $A_{HS}$ in Fig. 4(a). It is also interesting to note that the amplitude of the ultrafast MOKE signal taken by the two-color scheme rapidly diminishes when the temperature approaches $T_C$, as seen in the high temperature traces shown in Fig. 5(c). This corroborates the assignment of the overshoot in degenerate MOKE signals to the hole dynamics instead of the Mn spin dynamics.

## IV. CONCLUSIONS

In summary, we have successfully probed the previously-inaccessible non-equilibrium hole spin dynamics in ferromagnetic GaMnAs by using ultrafast MOKE spectroscopy. Below the Curie temperature $T_C$, an ultrafast linearly-polarized pump photoexcitation creates a non-equilibrium hole spin population via dynamical polarization of holes through exchange scattering with ferromagnetically-ordered Mn spins. This reveals the emergence of a new femtosecond relaxation component below $T_C$, which we attribute to hole spin lifetime $\tau_{HS}$ ~160-200 fs. This is clearly distinguished in the time domain from the much longer hole energy relaxation $\tau_{HE}$ ~1-2 ps, and from the Mn spin precession occurring on a 100-ps time scale. Our technique represents a new spectroscopy tool for studying non-equilibrium hole spins in magnetically ordered materials, which could be im-

portant in understanding the various collective behaviors and various forms of macroscopic order emerging in these systems. Additionally, our results have important implications for future applications of temporal spin effects in high speed spintronics that depend on hole-mediated ferromagnetism.

### Acknowledgments

Research supported by the National Science Foundation (NSF) under Award #DMR-1055352 (magneto-optical spectroscopy). Materials synthesis was supported by the National Science foundation Grant DMR1400432. This work was also supported by the European Unions Seventh Framework Programme (FP7- REGPOT-2012-2013-1) under grant agreement No. 316165 and by the EU Social Fund and National Resources through the THALES program NANOPHOS.

[1] H. Ohno, A. Shen, F. Matsukura, A. Oiwa, A. Endo, S. Katsumoto, and Y. Iye Applied Physics Letters **69**, 363-365 (1996).
[2] T. Li, A. Patz, L. Mouchliadis, J. Yan, T.A. Lograsso, I.E. Perakis, and J. Wang, Nature **496**, 69-73 (2013).
[3] A. Patz, T. Li, S. Ran, R.M. Fernandes, J. Schmalian, S.L. Bud'ko, P.C. Canfield, I.E. Perakis, and J. Wang, Nature Communications **5**, 3229 (2014).
[4] D.J. Hilton, and C.L. Tang, Phys. Rev. Lett **89**, 146601 (2002).
[5] S.P Dash, S. Sharma, R.M. Patel, M.P. de Jong, and R. Jansen, Nature **462**, 491-494 (2009).
[6] S. Iba, H. Saito, A. Spiesser, S. Watanabe, R. Jansen, S. Yuasa, and K. Ando Applied Physics Express **5**, 023003 (2012).
[7] Eiji Shikoh, Kazuya Ando, Kazuki Kubo, Eiji Saitoh, and Teruya Shinjo, Masashi Shiraishi, Phys. Rev. Lett. **110**, 127201 (2013).
[8] C. Hautmann, B. Surrer, and M. Betz, Phys. Rev. B **83**, 161203 (2011).
[9] Eric J. Loren, J. Rioux, C. Lange, J. E. Sipe, H. M. van Driel, and Arthur L. Smirl, Phys. Rev. B **84**, 214307 (2011).
[10] Claude Chappert, Albert Fert, and Frederic Nguyen Van Dau, Nat Mater **6**, 813-823 (2007).
[11] David D. Awschalom, and Michael E. Flatté, Nature Physics **3**, 153-159 (2007).
[12] I. Zutic, J. Fabian, and S. Erwin, J. Phys. Condens. Matter **19**, 165219 (2007).
[13] M. Dobrowolska, K. Tivakornsasithorn, X. Liu, J.K. Furdyna, M. Berciu, K.M. Yu,and W. Walukiewicz, Nature Materials **11**, 444-449 (2012).
[14] J. Wang, I. Cotoros, D.S. Chemla, X. Liu, J.K. Furdyna, J. Chovan,and I.E. Perakis, Appl. Phys. Lett. **94**, 021101 (2009).
[15] N. Tesarova, P. Nemec, E. Rozkotova, J. Zemen, T. Janda, D. Butkovicova,and F. Trojanek, K. Olejnk, V. Novak, P. Maly,and T. Jungwirth, Nature Photonics **7**, 492 (2013).
[16] M.D. Kapetanakis, P.C. Lingos, C. Piermarocchi, J. Wang, and I.E. Perakis, Appl. Phys. Lett. **99**, 091111 (2011). J. Opt. Soc. Am. B **29**, A95 (2012).
[17] M.D. Kapetanakis, I.E. Perakis, K.J. Wickey, C. Piermarocchi, and J. Wang, Phys. Rev. Lett. **103**, 047404 (2009).
[18] J. Wang, C. Sun, Y. Hashimoto, J. Kono, G. A. Khodaparast, Ł. Cywiński, L. J. Sham, G. D. Sanders, C. J. Stanton, and H. Munekata, J. Phys.: Condens. Matter **18**, R501 (2006).
[19] Ł. Cywiński and L. J. Sham, Phys. Rev. B **76**, 045205 (2007).
[20] J. Wang, C. Sun, J. Kono, A. Oiwa, H. Munekata, Ł. Cywiński, and L. J. Sham, Phys. Rev. Lett. **95**, 167401 (2005).
[21] J. Wang, I. Cotoros, K. M. Dani, D. S. Chemla, X. Liu, and J. K. Furdyna, Phys. Rev. Lett. **98**, 217401 (2007).
[22] J. Qi, Y. Xu, A. Steigerwald, X. Liu, J.K. Furdyna, I.E. Perakis, and N.H. Tolk Phys. Rev. B **79**, 085304 (2009).
[23] J. Qi, Y. Xu, N.H. Tolk, X. Liu, J.K. Furdyna, and I.E. Perakis, Appl. Phys. Lett. **91**, 112506 (2007).
[24] E. Rozkotova, P. Nemec, N. Tesarova, P. Maly, V. Novak, K. Olejnik, M. Cukr, and T. Junwirth, Appl. Phys. Lett. **93**, 232505 (2008).
[25] E. Rozkotova, P. Nemec, P. Horodyska, D. Sprinzl, F. Trojanek, P. Maly, V. Novak, K. Olejnik, M. Cukr, and T. Junwirth, Appl. Phys. Lett. **92**, 122507 (2008).
[26] A.V. Scherbakov, A.S. Salasyuk, A.V. Akimov, X. Liu, M. Bombeck, C. Bruggemann, D.R. Yakovlev, V.F. Sapega, J.K. Furdyna, and M. Bayer, Phys. Rev. Lett. **105**, 117204 (2010).
[27] Y. Hashimoto, S. Kobayashi, and H. Munekata, Phys. Rev. Lett. **100**, 067202 (2008).
[28] Y. Zhu X. Zhang, T. Li, L. Chen J. Lu,and J. Zhao, Appl. Phys. Lett. **94**, 142109 (2009).
[29] J. Wang, L. Cywiński, C. Sun, J. Kono, H. Munekata, and L.J. Sham, Phys. Rev. B **77**, 235308 (2008).
[30] B. Koopmans, M. van Kampen, J. T. Kohlhepp, and W. J. M. de Jonge, Phys. Rev. Lett. **85**, 844 (2000).
[31] J.P. Zahn, A. Gamouras, S. March, X. Liu, J.K. Furdyna, and K.C. Hall, J. Appl. Phys. **107**, 033908 (2010).
[32] K.C. Hall, J.P. Zahn, A. Gamouras, S. March, J.L. Robb, X. Liu, and J.K. Furdyna, Appl. Phys. Lett. **93**, 032504 (2008).
[33] K.J. Han, J.H. Yee, X. Liu, J.K. Furdyna,and F. Hache, Appl. Phys. Lett. **101**, 063519 (2007).
[34] In Fig. 4(a), the magnetization along the (001) axis is scaled so that at T=4K the magnetization component relates to a static polar Kerr angle of $\Theta_K$ ∼1.3mrad, as determined from the $\Theta_K$ measurement shown in Figure 1(b) for an external magnetic field of $B = 250mT$.
[35] K. Shen and M.W. Wu Phys. Rev. B. **85**, 075206 (2012).
[36] J. Szczytko, W. Bardyszewski, and A. Twardowski, Phys.

Rev. B **64**, 075306 (2001).
[37] Y. Zhang and S. Das. Sarma Phys. Rev. B. **72**, 125303 (2005).
[38] J. Wang, Y. Hashimoto, J. Kono, A. Oiwa, H. Munekata, G. D. Sanders, and C. J. Stanton, *Phys. Rev. B.* **72**, 153311 (2005).
[39] G. D. Sanders, C. J. Stanton, J. Wang, J. Kono, A. Oiwa and H. Munekata, *Phys. Rev. B.* **72**, 245302 (2005).
[40] E. Kojima, R. Shimano, Y. Hashimoto, S. Katsumoto, Y. Iye, and M. Kuwata-Gonokami, Phys. Rev. B **68**, 193203 (2003).